Purification and characterisation of the platelet-activating GPVI/FcRγ complex in SMALPs

Xueqing Wang [a,b,c,*], Alexandre Slater [b,d], Sarah C. Lee [a], Neale Harrison [a], Naomi L. Pollock [a], Saskia E. Bakker [e], Stefano Navarro [f,g], Bernhard Nieswandt [f,g], Tim R. Dafforn [a], Ángel García [c], Steve P. Watson [b,d], Michael G. Tomlinson [a,d,**]

[a] School of Biosciences, College of Life and Environmental Sciences, University of Birmingham, Birmingham B15 2TT, UK
[b] Institute of Cardiovascular Sciences, College of Medical and Dental Sciences, University of Birmingham, Birmingham B15 2TT, UK
[c] Centre for Research in Molecular Medicine and Chronic Diseases (CIMUS), Universidade de Santiago de Compostela, and Instituto de Investigación Sanitaria de Santiago (IDIS), 15782 Santiago de Compostela, Spain
[d] Centre of Membrane Proteins and Receptors (COMPARE), The Universities of Birmingham and Nottingham, The Midlands, UK
[e] School of Life Sciences, University of Warwick, Coventry CV4 7AL, UK
[f] Institute of Experimental Biomedicine I, University Hospital Würzburg, Würzburg Josef-Schneider-Straße 2, 97080 Wurzburg, Germany
[g] Rudolf Virchow Center for Integrative and Translational Bioimaging, University of Würzburg, 97080 Wurzburg, Germany

ARTICLE INFO

ABSTRACT

The collagen/fibrin(ogen) receptor, glycoprotein VI (GPVI), is a platelet activating receptor and a promising anti-thrombotic drug target. However, while agonist-induced GPVI clustering on platelet membranes has been shown to be essential for its activation, it is unknown if GPVI dimerisation represents a unique conformation for ligand binding. Current GPVI structures all contain only the two immunoglobulin superfamily (IgSF) domains in the GPVI extracellular region, so lacking the mucin-like stalk, transmembrane, cytoplasmic tail of GPVI and its associated Fc receptor γ (FcRγ) homodimer signalling chain, and provide contradictory insights into the mechanisms of GPVI dimerisation. Here, we utilised styrene maleic-acid lipid particles (SMALPs) to extract GPVI in complex with its two associated FcRγ chains from transfected HEK-293T cells, together with the adjacent lipid bilayer, then purified and characterised the GPVI/FcRγ-containing SMALPs, to enable structural insights into the full-length GPVI/FcRγ complex. Using size exclusion chromatography followed by a native polyacrylamide gel electrophoresis (PAGE) method, SMA-PAGE, we revealed multiple sizes of the purified GPVI/FcRγ SMALPs, suggesting the potential existence of GPVI oligomers. Importantly, GPVI/FcRγ SMALPs were functional as they could bind collagen. Mono-dispersed GPVI/FcRγ SMALPs could be observed under negative stain electron microscopy. These results pave the way for the future investigation of GPVI stoichiometry and structure, while also validating SMALPs as a promising tool for the investigation of human membrane protein interactions, stoichiometry and structure.

1. Introduction

Platelet collagen receptor glycoprotein VI (GPVI) plays an important role in platelet activation. At the site of blood vessel injury, GPVI binds collagen in the subendothelial matrix and induces downstream signalling events through the immunoreceptor tyrosine-based activation motifs (ITAMs) in its associated Fc receptor γ (FcRγ) disulphide-linked homodimer. The phosphorylated ITAMs then provide a docking site for the Syk non-receptor protein tyrosine kinase, initiating a downstream signalling cascade that activates the platelets [1]. More recently, GPVI has also been established as the receptor for fibrin(ogen), thus it is involved in the latter stages of thrombosis when firm thrombi involving multiple layers of platelets are formed [2,3]. Thus, GPVI is an attractive anti-thrombosis drug target and GPVI-blocking strategies are in clinical trials for the treatment of ischaemic stroke [2,4]. Indeed, it has been demonstrated that GPVI-deficient mice are protected against lethal

thromboembolism [5] and arterial thrombosis [6]. Moreover, a human population identified in Chile, lacking GPVI expression due to a missense mutation, have platelets which fail to aggregate on collagen, yet the affected people have only mild bleeding problems [7,8]. Therefore, GPVI is more important for the role of platelets in disease (thrombosis) than in preventing excessive blood loss upon injury (haemostasis). This is likely due to the relatively collagen-rich nature of atherosclerotic plaques, the rupture of which initiates arterial thrombosis.

Structurally, GPVI is a transmembrane protein with its extracellular region containing two immunoglobulin superfamily (IgSF) domains (D1 and D2) capable of recognising all of its known ligands, a mucin-like stalk region which is heavily O-glycosylated [9], a single transmembrane α-helix and cytoplasmic tail. GPVI and FcRγ interact via a salt bridge in their transmembrane regions [10]. Several structures of the GPVI IgSF domains have been solved so far. These include the original, dimeric structure of GPVI D1 and D2 domains, which shows a back-to-back dimer with the interface at the D2 domains [11]. In contrast, GPVI in complex with the D1-binding inhibitory nanobody Nb2 shows a dimeric structure in which D2 domains from two GPVI subunits form a domain-swapped dimer [12]. A third structure is a collagen-related peptide (CRP)-bound dimeric structure, showing back-to-back dimers with the interface at the D2 domains, similar to the original GPVI dimer structure [13]. CRP binds to the D1 domains, in a position close to the Nb2-binding groove, which indicates that the Nb2 inhibitory effect could be due to allosteric modulation or steric clash [12,13]. A fourth structure is another GPVI inhibitory nanobody, Nb35-bound structure, which shows a monomeric conformation of GPVI, while arrangement of D1 and D2 domains is comparable to that in the original dimeric GPVI [14]. Notably, all these solved structures involve only GPVI D1 and D2 domains; structural information involving the glycosylated stalk, the transmembrane helix, the cytoplasmic tail and the FcRγ chains are therefore currently lacking. Moreover, it remains unknown if the GPVI dimers represent the dimers in the membrane or if they are crystallographic artefacts. There is controversy in the literature over whether the GPVI dimer represents a biologically active form of the receptor, with a unique ligand-binding epitope, in comparison to the monomer [15–17]. To better understand the mechanism and functional significance of GPVI dimerisation, a full-length GPVI structure, ideally in complex with the FcRγ, would be beneficial, as the regions other than the two IgSF domains could potentially introduce steric constraints and refinement to their spatial arrangements. In addition, the structure of full-length GPVI in complex with FcRγ in its native lipid environment could help explain the mechanism of GPVI clustering upon binding agonists, thus providing insights into the downstream signalling events.

It is challenging to extract transmembrane proteins from their native lipid bilayer environment without destroying their bioactive structures and interactions, as traditionally-purified detergent-micelle-encapsulated membrane proteins can easily be destabilised [18]. Moreover, the extracting procedures typically involve tedious screening of detergents and buffers [19]. To address these problems, a novel strategy utilising styrene maleic acid lipid particles (SMALPs), has been recently developed. SMA co-polymers have been utilised to excise patches out of native membranes, generating nanodiscs directly from the membrane bilayer without the involvement of detergents in any of the steps [19,20]. SMALPs are disc-shaped, containing the native arrangement of the lipid bilayer and the membrane proteins embedded inside, are ~10 nm in diameter and readily amenable to many biochemical and biophysical applications [18,21].

In this work, the SMALP technology was applied to the extraction and characterisation of the GPVI/FcRγ complex from a human cell line over-expression system, with an ultimate goal to develop materials and methodologies for the structural determination of full-length GPVI in complex with FcRγ.

2. Materials and Methods

2.1. Plasmids

Human GPVIa-10xHis and GPVIb-10xHis were generated by PCR from pcDNA3-human GPVIa-myc and GPVIb-myc vectors [22] with primers 5′-TAGTAGGATCCACCATGTCTCCATCCCCGAC-3′ and 5′-TAGTAGGCGGCCGCTCAGTGGTGGTGATGATGGTGATGGTGGTGGTG-TGAACATAACCCGCGGCTGTG-3′, followed by subcloning into the pEF6/myc-His C expression vector; inclusion of a stop codon in the primer was designed to prevent expression of the myc and His tags from the vector. The pEF6-FcRγ plasmid was as described in Ref. [22].

pEF6-GPVIa-Δexon5-10xHis and pEF6-GPVIb-Δexon5-10xHis were then generated by a two-step PCR process from pEF6-GPVIa-10xHis and pEF6-GPVIb-10xHis, using primers 5′- CCCTGGAGCTTGTGGTCACA-GAATTCTCAGAAGCCACCGC-3′ and 5′- GCGGTGGCTTCTGA-GAATTCTGTGACCACAAGCTCCAGGG-3′ to amplify Δexon5 GPVI.

2.2. Cell culture and transfection

The human embryonic kidney (HEK)-293T (HEK-293 cells expressing the large T antigen of simian virus 40) cell line, with a disintegrin and metalloprotease 10 (ADAM10) knocked out by CRISPR/Cas9 [23], was cultured in Dulbecco's Modified Eagle Medium (DMEM) (Merck) supplemented with 10% fetal bovine serum (Thermo Fisher Scientific), 4 mM L-glutamine, 100 U/ml penicillin and 100 μg/mL streptomycin (Merck). Cells were transiently transfected with polyethylenimine (Merck) as described [24]. For the expression level comparison of different GPVI constructs, 0.5 μg of pEF6-GPVI-10xHis and 0.5 μg of pEF6-FcRγ were transfected for each well in a 6-well plate (35 mm in diameter). The amount of DNA for larger-scale transfections is stated in later sections.

The DT40 chicken B cell line was cultured in Roswell Park Memorial Institute Medium (RPMI) (Merck) supplemented with 10% fetal bovine serum (Thermo Fisher Scientific), 4 mM L-glutamine, 100 U/ml penicillin, 100 μg/mL streptomycin and 50 μM β2-mercaptoethanol (Merck). DT40 cells were transiently transfected by electroporation before NFAT-luciferase transcriptional reporter assay as described [22]. For each transfection, 1.5×10^7 cells, 20 μg NFAT-luciferase reporter [22], 0.25 μg pEF6-GPVI-10xHis and 0.25 μg pEF6-FcRγ were used. All cells were grown in a humidified incubator at 37 °C with 5% CO_2.

2.3. Flow cytometry

For flow cytometry of GPVI, cells were stained with 10 μg/mL mouse anti-human GPVI monoclonal antibody HY101 (eBioscience) or isotype control MOPC-21 mouse IgG1 (Merck), followed by fluorescein isothiocyanate (FITC)-conjugated sheep anti-mouse IgG (Thermo Fisher Scientific). Samples were processed on a FACSCalibur flow cytometer and data collected and analysed using CellQuest Pro software (BD Biosciences).

2.4. SMALP preparation and purification from HEK-293T cells

One hundred 15 cm plates of adherent ADAM10 knockout HEK-293T cells [23] were transfected with 9 μg of pEF6-GPVIa-10xHis and 9 μg of pEF6-FcRγ per plate [22], harvested two days later and cell pellets preserved at −80 °C until use. Approximately 8 mL of cell pellet was collected. To generate GPVI/FcRγ SMALPs, cells were defrosted on ice, resuspended in 50 mL buffer containing 50 mM Tris pH 8, 2 mM EDTA, 5 % glycerol, containing one tablet of cOmplete™ Mini Protease Inhibitor Cocktail (Merck), and homogenised with a Dounce homogeniser. The homogenised cells were passed through a C3 machine for four rounds, with air supply being approximately 40 psi, and the actual pressure on cells being 10,000–15,000 psi for the cells to be disrupted. Membranes were separated from cell debris by centrifuging at $8200 \times g$ for 30 min at

4 °C. The supernatant was collected and membrane pelleted from it by ultracentrifugation at $100,000 \times g$ for 1 h at 4 °C. The pelleted membrane was resuspended in 50 mM Tris pH 8, 500 mM NaCl, 10 % glycerol (SMALPing buffer) to 40 mg/mL and homogenised with a Dounce homogeniser. SMALP 30010P (Orbiscope) was added to the membrane resuspension to a final concentration of 2.5% (wt [g]/vol [mL]), and incubated at room temperature for 2 h. SMALP particles were further purified by removing debris material by ultracentrifugation at $100,000 \times g$ for 1 h at 4 °C, and the supernatant containing SMALPs was retained. SMALPs in solution were incubated with 5 mL of Ni-NTA beads (50% slurry) (Generon) at room temperature for 48 h to maximise binding. To ensure optimum recovery of SMALPs, the process was repeated by resuspending the pellet in the last round of ultracentrifugation to 40 mg/mL in SMALPing buffer with 2.5% SMALP 30010P. In this further round of purification, solutions containing SMALPs were incubated with 3 mL of Ni-NTA beads (50% slurry) at room temperature for 24 h.

Purification using the 10 *x* His-Tag was undertaken by gravity flow. Briefly, the Ni-beads bound to GPVI/FcRγ SMALPs were combined into one column, resulting in 8 mL of 50% slurry beads. Beads were washed in one column volume of SMALPing buffer twice, in one column volume of SMALPing buffer supplemented with 10 mM imidazole once, in one column volume of SMALPing buffer supplemented with 20 mM imidazole once, followed by four 1.5 mL elutions with 500 mM imidazole in SMALPing buffer. Samples in each step were collected and loaded on SDS-PAGE. Samples containing GPVI/FcRγ SMALPs were identified and combined, dialysed in 3.5 kDa MWCO mini dialysis devices (Thermo Fisher Scientific), concentrated by a Vivaspin 5000MWCO concentrator (GE Healthcare) at $3000 \times g$, 4 °C to 500 μL, and subjected to size exclusion chromatography.

2.5. Size exclusion chromatography

GPVI/FcRγ SMALPs were further purified using fast pressure liquid chromatography (FPLC) with an ÄKTA pure system with a Superdex 200 increase 10/300 column attached (Cytiva). The column was equilibrated in SMALPing buffer. SMALPing buffer was loaded through a 500 μL loop. The ÄKTA pure was run at 0.5 mL/min, and 500 μL fractions were collected.

2.6. SDS-PAGE

Samples were mixed with 2*x* Laemmli sample buffer or NuPAGE™ LDS sample buffer (Thermo Fisher Scientific), in either non-reduced or reduced conditions, as indicated in each experiment. Samples in Laemmli sample buffer were heated at 95 °C for 5 min for the proteins to be denatured and coated with SDS, while samples in NuPAGE™ LDS sample buffer were heated at 70 °C for 10 min. The boiled samples were loaded into polyacrylamide gels, either handmade or precast NuPAGE™ gels. Electrophoresis was performed in the XCell SureLock™ Mini-Cell system (Thermo Fisher Scientific).

2.7. SMA-PAGE

SMA-PAGE was performed as previously described [25]. Briefly, SMALPs in solution were mixed with 4*x* Native sample buffer (Thermo Fisher Scientific) and loaded onto Mini-PROTEAN® TGX™ Precast Protein Gels (Bio-Rad Laboratories), without being boiled. The running buffer was composed of 25 mM Tris and 192 mM glycine. Electrophoresis was performed in the Mini-PROTEAN Tetra Cell system (Bio-Rad Laboratories).

2.8. Western blotting

SDS-PAGE gels were transferred in an XCell II™ Blot Module (Thermo Fisher Scientific), onto Immobilon®-FL PVDF membrane

(Millipore), at room temperature, 30 V for 90 min. Membranes were blocked using 3% BSA in 20 mM Tris pH 7.6, 137 mM NaCl, 0.1% Tween-20 (TBST), for 1 h at room temperature. Primary antibody probing was done in 3% BSA in TBST overnight at 4 °C, with one of the following antibodies: anti-GPVI 11A7 at 0.5 μg/mL (a gift from Elizabeth Gardiner, Australian National University [26]), anti-GPVI Emf-1 at 0.5 μg/mL (kindly provided by EMFRET Analytics (Eibelstadt, Germany) [27]), or anti-FcRγ at 1:2000 dilution (Sigma-Aldrich). Secondary antibody probing was done in 3% BSA in TBST with IRDye-conjugated antibody (LI-COR Biosciences), for 2 h at room temperature.

SMA-PAGE gels were first soaked in SDS-PAGE running buffer (25 mM Tris, 192 mM glycine, 0.1% SDS) for 10 min at room temperature with agitation, for the protein surfaces to be coated with SDS to facilitate transferring, then briefly soaked in transfer buffer (25 mM Tris, 192 mM glycine, 20 % methanol) before transferring to PVDF membrane. Membranes were incubated in 5% BSA in TBST with 25 mM L-arginine to prevent nonspecific binding. These membranes were then processed in the same way as for Western blotting of SDS-PAGE. For imaging, the membrane was dried with filter paper and scanned on the LI-COR Odyssey Infrared Imaging System (LI-COR Biosciences).

2.9. Gel staining

For Coomassie staining, the gel was briefly washed in H_2O, stained in Coomassie blue R-250 staining solution (50% methanol, 10% acetic acid, 0.05% w/v Coomassie Blue R250 (Thermo Fisher Scientific)) prewarmed at 40 °C, for a few hours until the whole gel was stained blue, and destained in 30% methanol, 7% acetic acid. Silver stain was performed with Pierce™ Silver Stain Kit (Thermo Fisher Scientific) following the manufacturer's instructions.

2.10. Collagen agarose binding assay

Collagen agarose (Sigma-Aldrich) was washed in SMALPing buffer and resuspended to a 50% slurry. 20 μL of slurry was added to 1 mL of GPVI/FcRγ-SMALPs in solution. Samples were incubated at room temperature with rotation for 90 min, followed by three washes with 1 mL SMALP buffer. Samples were then further analysed by SDS-PAGE.

2.11. Negative stain electron microscopy

Samples were applied to a glow-discharged, carbon/formvar coated grid (EM Resolutions) and stained with 2% uranyl acetate for 1 min. Grids were imaged using the JEOL 2100Plus (JEOL, Japan) with Gatan OneView camera (Gatan/Ametek, USA) at 40,000 magnification. 2D class averages were produced using Relion [28].

2.12. Mass spectrometry

Detection of in-gel proteins by mass spectrometry was performed as previously described [29]. Briefly, protein bands of interest from silver stained SDS-PAGE gels were excised out, then the gel fractions were subjected to trypsin digestion, followed by liquid chromatography and tandem mass spectrometry (LC-MS/MS) via a QExactive HF mass spectrometer (Thermo Fisher Scientific). The MS and MS/MS scans were searched against the Uniprot database using Proteome Discoverer 2.2 (ThermoFisher Scientific).

3. Results

3.1. GPVI isoforms GPVIa, GPVIb and Δexon5 exhibit similar expression levels and collagen receptor function in transfected cells

GPVI has two major isoforms, GPVIa and GPVIb, and the shorter isoform lacking 18 amino acids within the O-glycosylated stalk (Δexon5). There have been contradictory results on the relative

expression levels and clinical impact of GPVIa and GPVIb [30–33], and the Δexon5 versions have not previously been compared for expression levels and collagen receptor function. In addition, comparing the full-length and Δexon5 constructs could provide insight into the role of the glycosylated stalk. In order to identify which construct yields the highest expression levels, His-tagged expression constructs were generated for GPVIa, GPVIb and the Δexon5 version of each (Fig. 1). To determine their expression levels, the four expression constructs were transiently transfected into HEK-293T cells, which do not express endogenous GPVI. Flow cytometry with a GPVI monoclonal antibody (mAb) showed that all four GPVI constructs had comparable surface expression levels, as judged by relative geometric mean fluorescence intensity (gMFI) of transfected cells and percentage of cells transfected (Fig. 2A), albeit different cells had different GPVI surface expression levels due to the nature of transient transfection. Western blotting of whole cell lysates showed that all four GPVI constructs had comparable whole cell expression levels (Fig. 2B). As exon 5 encodes for 18 amino acids within the mucin-like stalk region which is heavily O-glycosylated [9], and there are three putative O-glycosylation sites within the 18 amino acids [34], the molecular weight difference between the full-length and Δexon5 versions of GPVI was 5–7 kDa (Fig. 2B).

To determine whether the GPVI isoforms are functional in terms of signalling in response to collagen, each construct was transfected into the DT40 model B cell line together with an NFAT-luciferase transcriptional reporter construct, which is an established system to measure GPVI signalling [22]. Collagen-induced NFAT activation was similar for all four isoforms (Fig. 3A), and they expressed at similar levels on the DT40 cell surface (Fig. 3B).

Together, these data suggest no expression or signalling differences between GPVIa, GPVIb and Δexon5 variants in transfected cells. Therefore, for the expression and purification in the remainder of this study, the best-studied GPVIa including exon 5 was selected.

3.2. Purification of GPVI-SMALPs

To generate and purify GPVI SMALPs, the plasmids expressing GPVIa-His and FcRγ were transiently transfected into HEK-293T cells, the latter being ADAM10 knockout [23] to prevent the constitutive GPVI cleavage by ADAM10 that was previously demonstrated in HEK-293T cells [35]. Expression of GPVI was confirmed by flow cytometry (Fig. 4A). Cells were stored at −80 °C immediately after harvesting until use. On the day of generating SMALPs, ~8 mL centrifuged volume of cells were defrosted on ice, membranes isolated and SMALPed using SMALP 30010P (Orbiscope). After the first round of exposure to SMA,
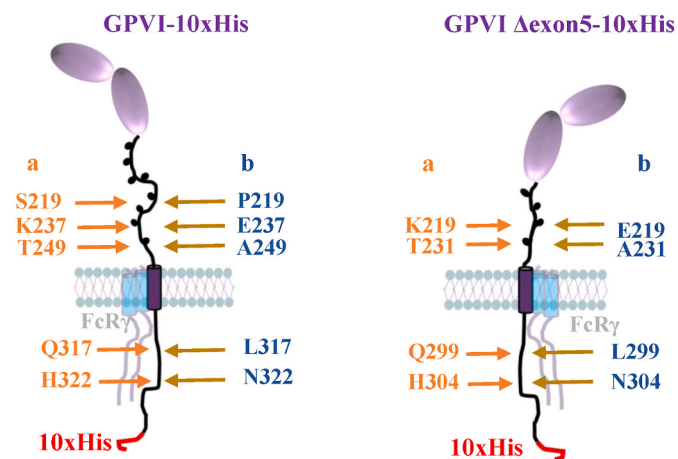
the remaining pellet was again solubilised using SMALP 30010P to maximise SMALP recovery. The generated SMALPs were then purified by incubating with Ni-NTA beads and eluting with imidazole. Analyses of samples from the purification procedure by SDS-PAGE demonstrated successful purification of a major protein band at the predicted molecular weight of GPVI by Coomassie and silver stain (Fig. 4Bi-ii), and GPVI Western blotting confirmed the presence of GPVI (Fig. 4Biii).

3.3. Size exclusion chromatography of GPVI/FcRγ SMALPs reveals distinct populations of GPVI oligomers

The purified SMALPs were further separated by size using a Superdex 200 10/300 Increase column in SMALPing buffer. The resulting profile demonstrated a wide peak which appeared immediately after the void volume (Fig. 5A). Western blotting confirmed the presence of GPVI and FcRγ in fractions 4–14 (Fig. 5B). Under non-reduced conditions, a GPVI blot revealed the existence of GPVI dimers and high molecular weight species; the latter are likely to represent GPVI oligomers within the same SMALPs or aggregation of several GPVI-containing SMALPs (Fig. 5B). This suggests full-length GPVI forms disulphide-linked dimers which has previously been proposed [36]. FcRγ blots revealed the presence of FcRγ dimers under non-reducing conditions which were reduced to monomers under reducing conditions. Nevertheless, the co-elution of GPVI and FcRγ (Fig. 5B) suggests that FcRγ and GPVI express as a complex in the transiently transfected HEK-293T cells, and they can be isolated together within the same particle.

Next, a novel native PAGE method, SMA-PAGE, which was specifically developed for SMALPs by Pollock et al. [25], was applied to further characterise the molecular weights of the entire SMALPs. SMA-PAGE utilises the unique negatively charged belt, the SMA polymer, as the driving force in PAGE, instead of the traditionally-used SDS, thus the migration of intact SMALP particles on PAGE can be achieved without the addition of any other chemicals apart from the native sample buffer. Interestingly, when the size exclusion chromatography (SEC) fractions were loaded onto SMA-PAGE, followed by Western blotting against GPVI and FcRγ, each fraction was identified as a single diffuse band, with the molecular weight decreasing from the early fractions to the later ones, spanning from above 720 kDa–~70 kDa which corresponds to GPVI plus FcRγ dimer (Fig. 5C). The major peak in fractions 4 and 5 consisted of a large complex at approximately 500–700 kDa. The later fractions (fractions 9–14) are likely more homogeneous as they were less diffuse (Fig. 5C). Moreover, the bands all overlayed between GPVI and FcRγ blots, a further confirmation that GPVI and FcRγ form a complex and exist in the same SMALPs. The SMA-PAGE results suggest that GPVI/FcRγ in SMALPs from HEK-293T cells possibly comprise different oligomeric states of the GPVI/FcRγ complexes.

3.4. GPVI and FcRγ are the predominant protein components in the purified SMALPs

To assess the purity of the GPVI/FcRγ SMALP samples, the SEC fractions were run on SDS-PAGE and silver stained. Three major bands were detected at approximately 100 kDa, 57 kDa and 18 kDa (Fig. 6). These were excised from the silver-stained gel and subjected to liquid chromatography followed by tandem mass spectrometry (LC-MS/MS). This revealed GPVI as the most abundant species for the ~100 kDa and the ~57 kDa bands, suggesting GPVI dimers and monomers, respectively, and FcRγ as the most abundant species for the ~18 kDa band, suggesting an FcRγ dimer (Supplementary Tables 1–3). These results demonstrate that the purified SMALPs are relatively pure, with GPVI and FcRγ being the main protein components.
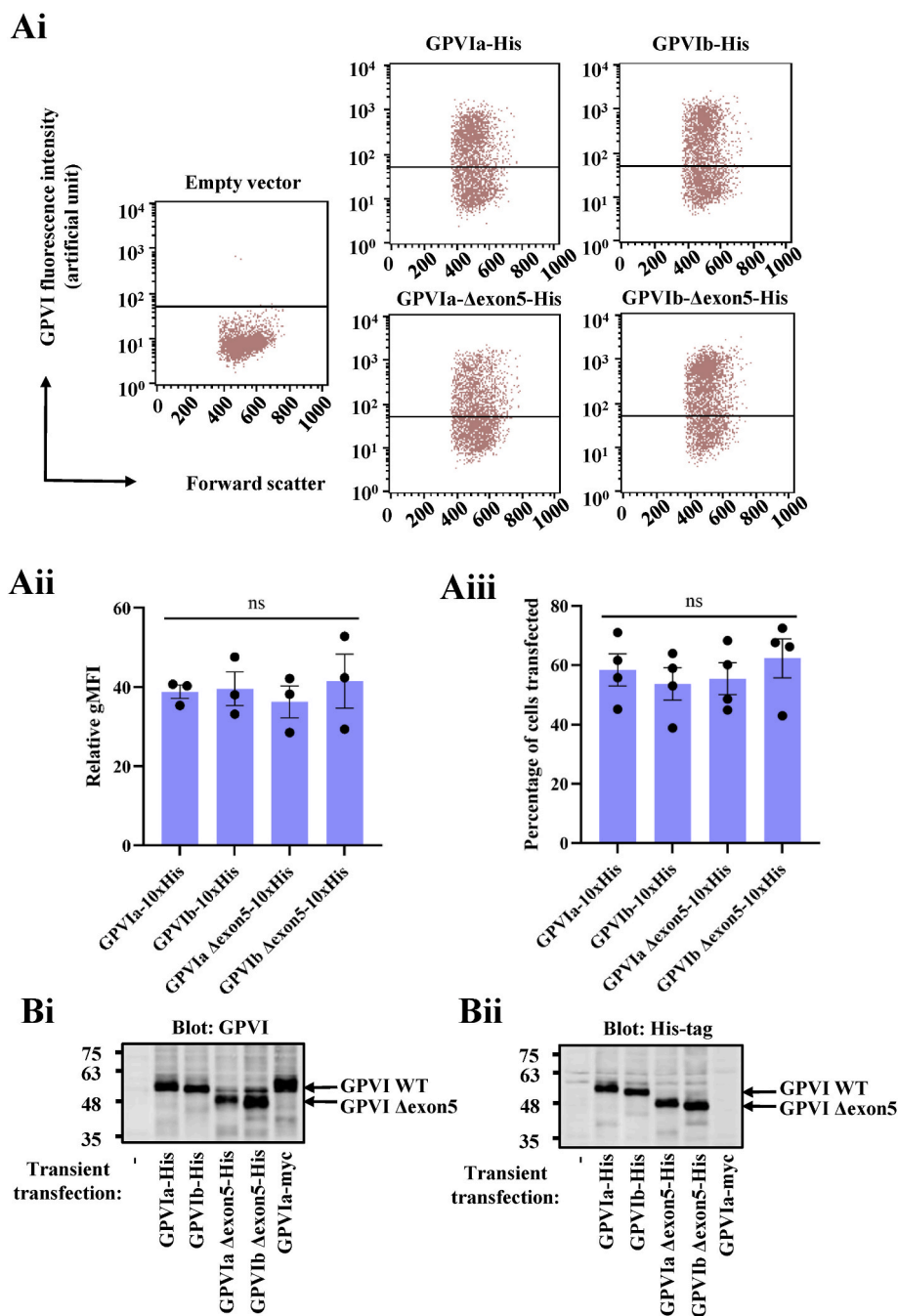

Fig. 1. Structural illustration of the four GPVI isoforms with 10x His tags. The cartoon illustration of GPVI structures, with the different amino acids in allelic isoforms a and b labelled. The detailed sequence information is in Supplementary Fig. 1.

Fig. 2. The four GPVI-10xHis constructs have comparative surface and whole-cell expression levels when transiently transfected into HEK-293T cells.
(Ai) HEK-293T cells were transiently transfected with empty vector control or the indicated His-tagged GPVI and FcRγ expression constructs, and cell surface GPVI was detected by flow cytometry with GPVI monoclonal antibody HY101 followed by FITC-conjugated anti-mouse secondary antibody. The plots shown are representative of four independent experiments. (Aii) Relative GPVI expression was quantified by dividing the geometric mean of fluorescence intensity (gMFI) of the GPVI-transfected by the gMFI of the empty vector negative control. (Aiii) The percentage of transfected cells was quantified. Error bars represent the standard error of the mean. (B) Transfected cells from (A) were lysed in 1% Triton X-100 lysis buffer and lysates subjected to Western blotting with (Bi) anti-GPVI antibody 11A7 and (Bii) anti-His antibody. The blots shown are representative of two independent experiments.

### 3.5. Mono-dispersed particles of GPVI/FcRγ SMALPs identified with negative stain EM

To visualise the purified GPVI/FcRγ SMALPs, fractions 5, 7 and 10 from SEC were chosen as representatives for possible high-, medium- and low-order oligomers for negative stain EM. Amongst the images, those from fraction 7 showed clearly mono-dispersed, protein-like particles (Fig. 7A). 2D classification was performed from ~1,000 particles on the images collected from fraction 7, where 39 class averages were generated (Fig. 7B). The averages were ranked by the number of particles in the corresponding classes with the frequencies calculated (Fig. 7C). However, the number of particles was too low for 3D structure construction.
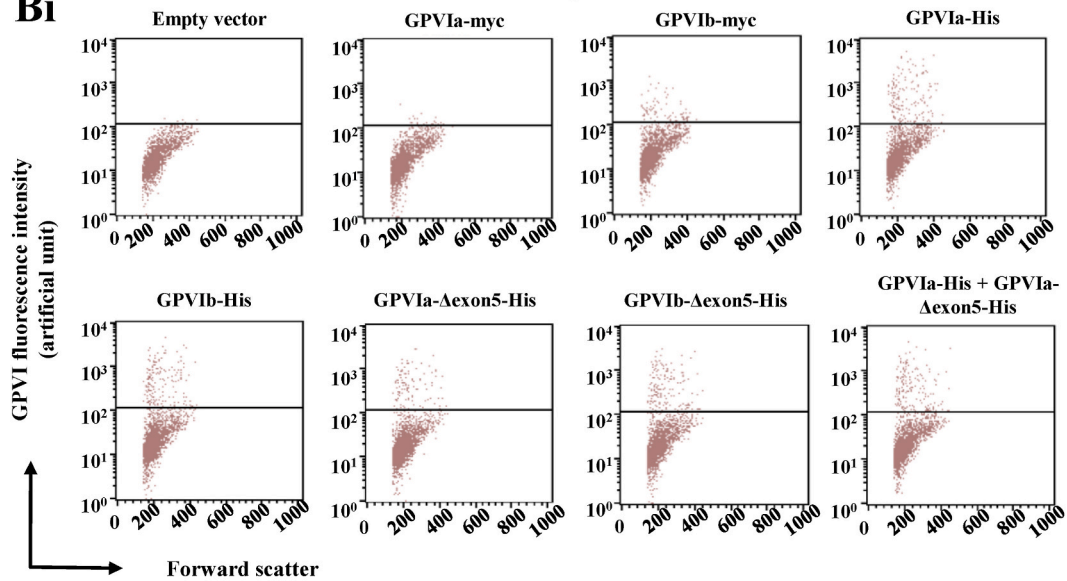
3.6. GPVI/FcRγ SMALPs bind collagen

To evaluate whether GPVI/FcRγ encapsulated in SMALPs remains functional, a collagen pull-down assay was performed. The SEC fractions
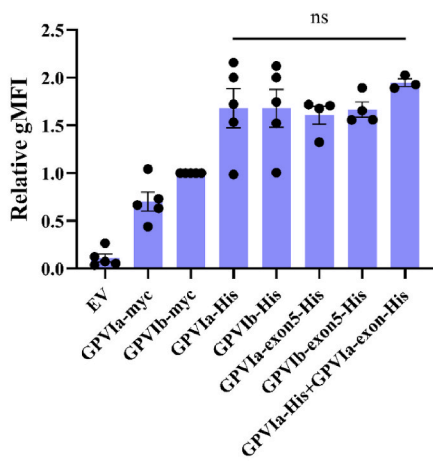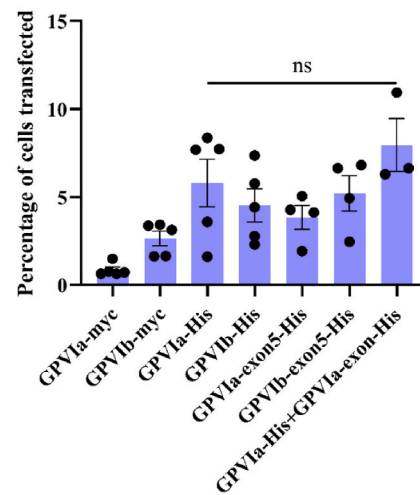
A
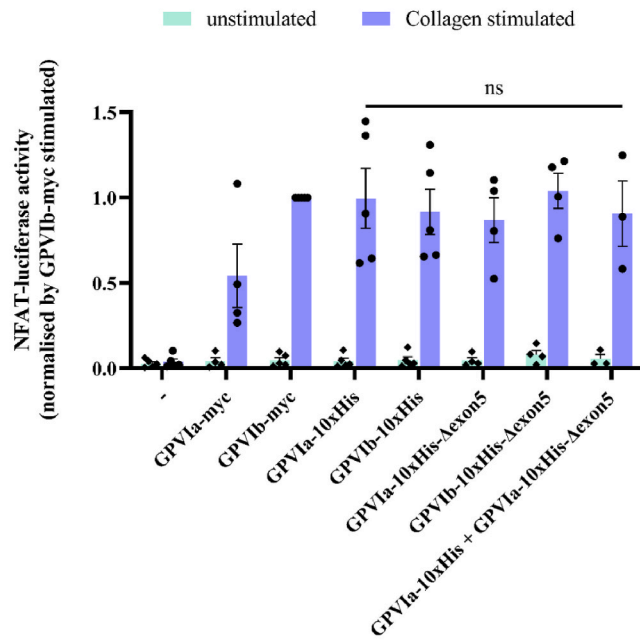
Bi

Bii

Biii

(caption on next page)

Fig. 3. The four GPVI-10xHis constructs have comparative downstream signalling levels shown by an NFAT-luciferase reporter assay.
(A) DT40 cells were transfected with NFAT-luciferase reporter, indicated GPVI isoform and FcRγ, stimulated with 5 µg/mL of Horm collagen, then subjected to luciferase reporter assay. Luciferase activity was measured after luciferin injection. The luminometer readout of unstimulated or collagen-stimulated was presented after normalised by the readout of collagen-stimulated, GPVIb-myc transfected cells. Error bars represent the standard error of the mean from five independent experiments. (Bi) GPVI surface expression were measured by flow cytometry, with GPVI monoclonal antibody HY101 followed by FITC-conjugated anti-mouse antibody. The plots shown are representative from six independent experiments. (Bii) Relative GPVI expression were quantified by dividing the geometric mean of fluorescence intensity (gMFI) of the GPVI-transfected cells by the gMFI of the empty vector negative control. Error bars represent the standard error of the mean from four independent experiments. (Biii) The percentage of transfected cells was quantified. Error bars represent the standard error of the mean from five independent experiments.
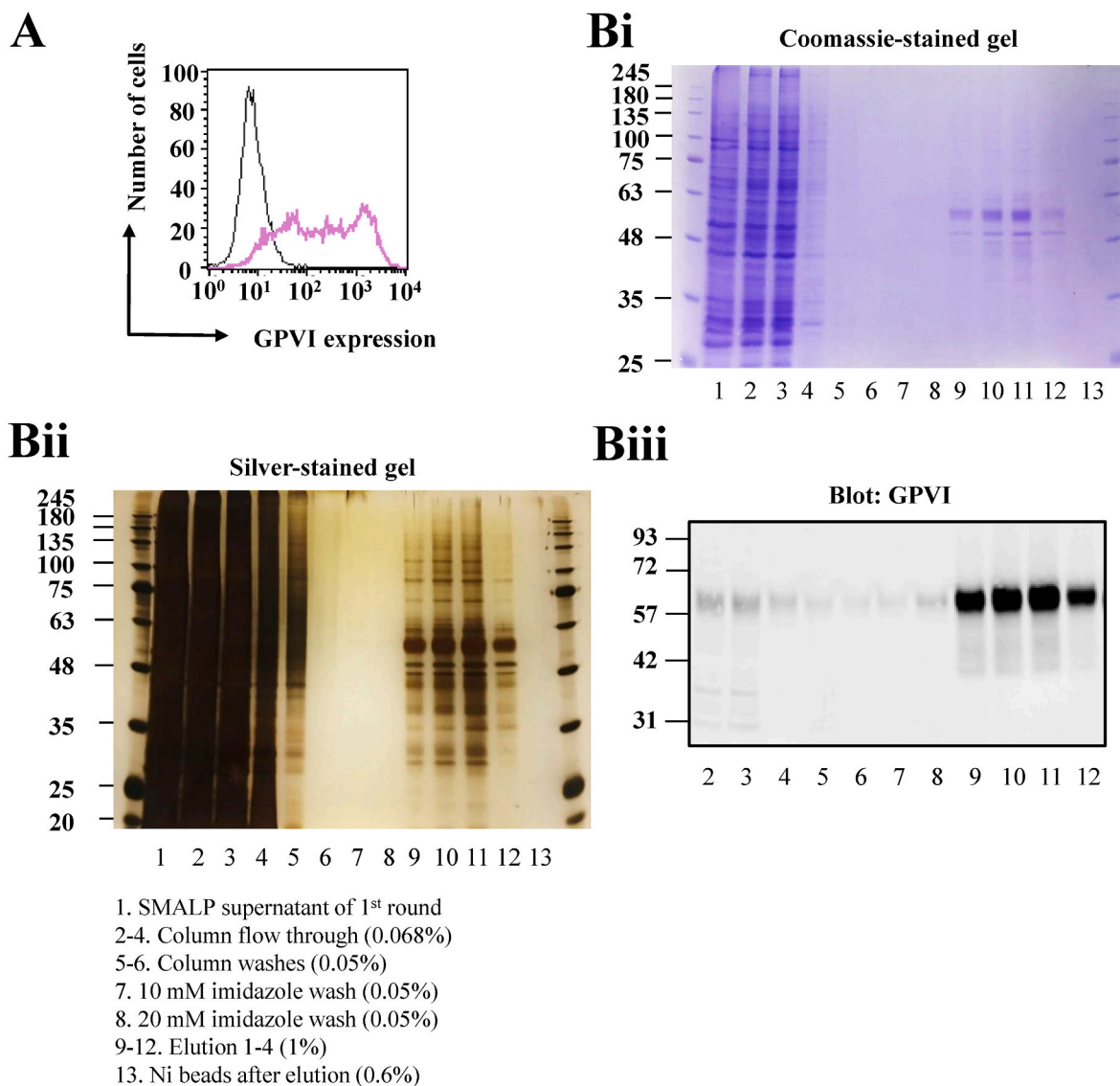

1. SMALP supernatant of 1st round
2-4. Column flow through (0.068%)
5-6. Column washes (0.05%)
7. 10 mM imidazole wash (0.05%)
8. 20 mM imidazole wash (0.05%)
9-12. Elution 1-4 (1%)
13. Ni beads after elution (0.6%)

Fig. 4. Purification of GPVIa-His SMALPs.
(A) ADAM10-knockout HEK-293T cells were transfected with GPVIa-His and FcRγ expression constructs, and two days later analysed by flow cytometry with GPVI mAb HY101 followed by FITC-conjugated anti-mouse secondary antibody. The magenta trace represents GPVI staining, and the black trace represents the isotype-matched MOPC-21 negative control mAb. (B) GPVIa-10xHis was transfected into and expressed in HEK-293T cells (from 100 confluent 15 cm-plates) and GPVIa-His SMALPs purified as described in Materials and Methods. For maximum solubilisation efficiency, the non-SMALPed debris from the first round of SMALP generation was collected and incubated with SMA, and the generated SMALPs were affinity purified via gravity column. Purified SMALPs from both rounds were combined for downstream characterisation. The indicated fractions from the purification procedure were analysed by Coomassie stain (Bi), silver stain (Bii) and Western blotting with anti-GPVI monoclonal antibody, Emf-1 (Biii). The percentage of each fraction that was loaded onto the gel was indicated in parentheses, i.e. 0.05% of column wash was loaded onto the gel.

were pooled into three groups—fraction 4–6, fraction 7–9 and fraction 10–13, potentially demonstrating high-, medium- and low-order oligomers, and pulled down by collagen-conjugated agarose beads. GPVI blot revealed efficient pull-down in all three groups (Fig. 8A), while similar quantities of input GPVI for each of the three pull-downs were confirmed by GPVI Western blotting (Fig. 8A). As a further confirmation of collagen binding, GPVI/FcRγ SMALPs from a separate preparation were incubated together with Horm collagen, and the mixture in SMALPing buffer
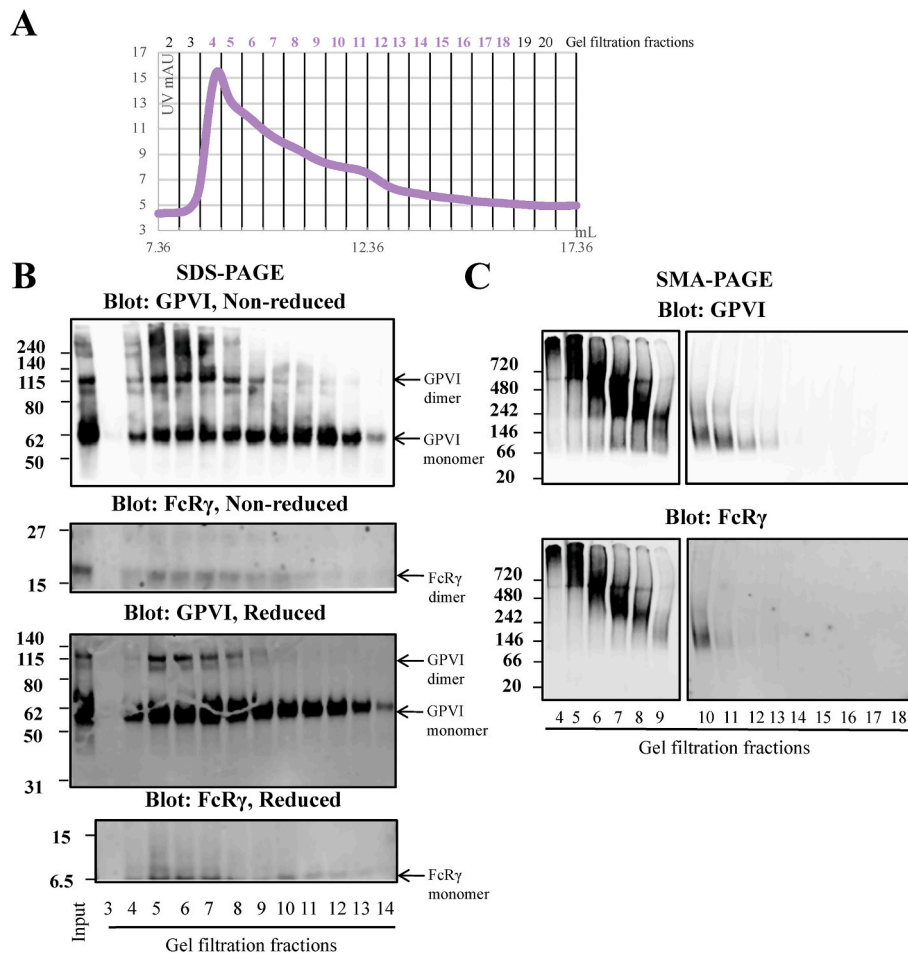
Fig. 5. Gel filtration of GPVI/FcRγ SMALPs reveals distinct populations of GPVI oligomers.
(A) Superdex 200 10/300 Increase column gel filtration profile of the pooled, dialysed and concentrated GPVI-SMALP elutions from Ni-NTA affinity column. Numbers on upper x-axis refer to the number of the fractions collected. (B) SDS-PAGE and (C) native SMA-PAGE of gel filtration fractions followed by Western blotting for GPVI and FcRγ.
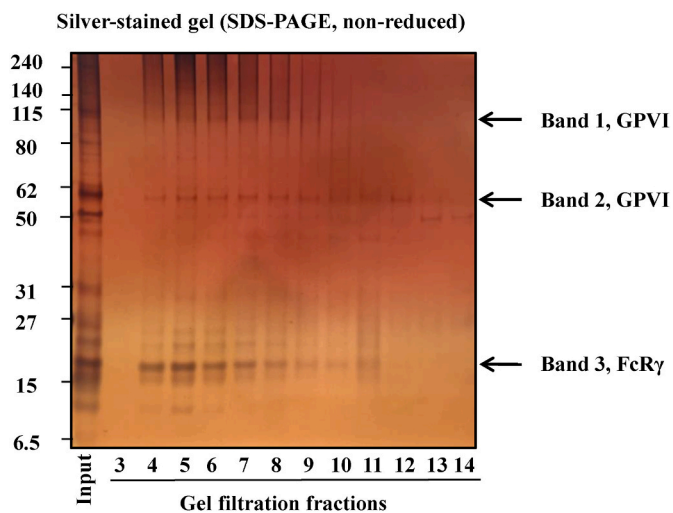

Fig. 6. The purified GPVI/FcRγ SMALPs are relatively pure.
GPVI SMALP gel filtration fractions were analysed by SDS-PAGE followed by silver stain. The three main bands, at approximately 100 kDa, 57 kDa and 18 kDa, were excised and analysed by LC-MS/MS, and the major species identified were indicated by the arrows. Band 1 was excised from fractions 4–9, band 2 was excised from fractions 4–11, and band 3 was excised from fractions 4–9.

was applied onto negative stain EM grids. The images showed clearly visible thick and thin collagen fibres, with round, nanodisc-like objects attached to them (Fig. 8B). These results provide evidence that GPVI in SMALPs is properly folded and functional in binding collagen.

4. Discussion

In this work, full-length GPVI in complex with FcRγ was successfully extracted into SMALPs, following expression in a transiently transfected human cell line, HEK-293T. GPVI/FcRγ SMALPs purified with affinity chromatography using Ni-NTA beads and gravity flow, followed by FPLC SEC showed a wide size distribution, possibly comprising the GPVI/FcRγ complex with different oligomeric states. The purified SMALPs contained GPVI and FcRγ as the major protein components. In addition, mono-dispersed particles of the purified GPVI/FcRγ SMALPs were observed under negative stain EM. Moreover, functional activity of the GPVI/FcRγ in SMALPs with different sizes was demonstrated by their ability to bind to collagen, as shown by both *in vitro* binding assay and negative stain EM. This is the first report of purifying GPVI/FcRγ with lipid nanodiscs, demonstrating that SMALPs are a promising tool for the investigation of platelet receptor stoichiometry and structure.

The SEC profile in this work potentially demonstrated two major peaks for purified GPVI/FcRγ SMALPs, with the first one immediately after the void volume and the second one in between fractions 11–12, which were connected by a series of middle-sized particles, represented as the slope between the two peaks (Fig. 5A, fractions 5–10). A similar
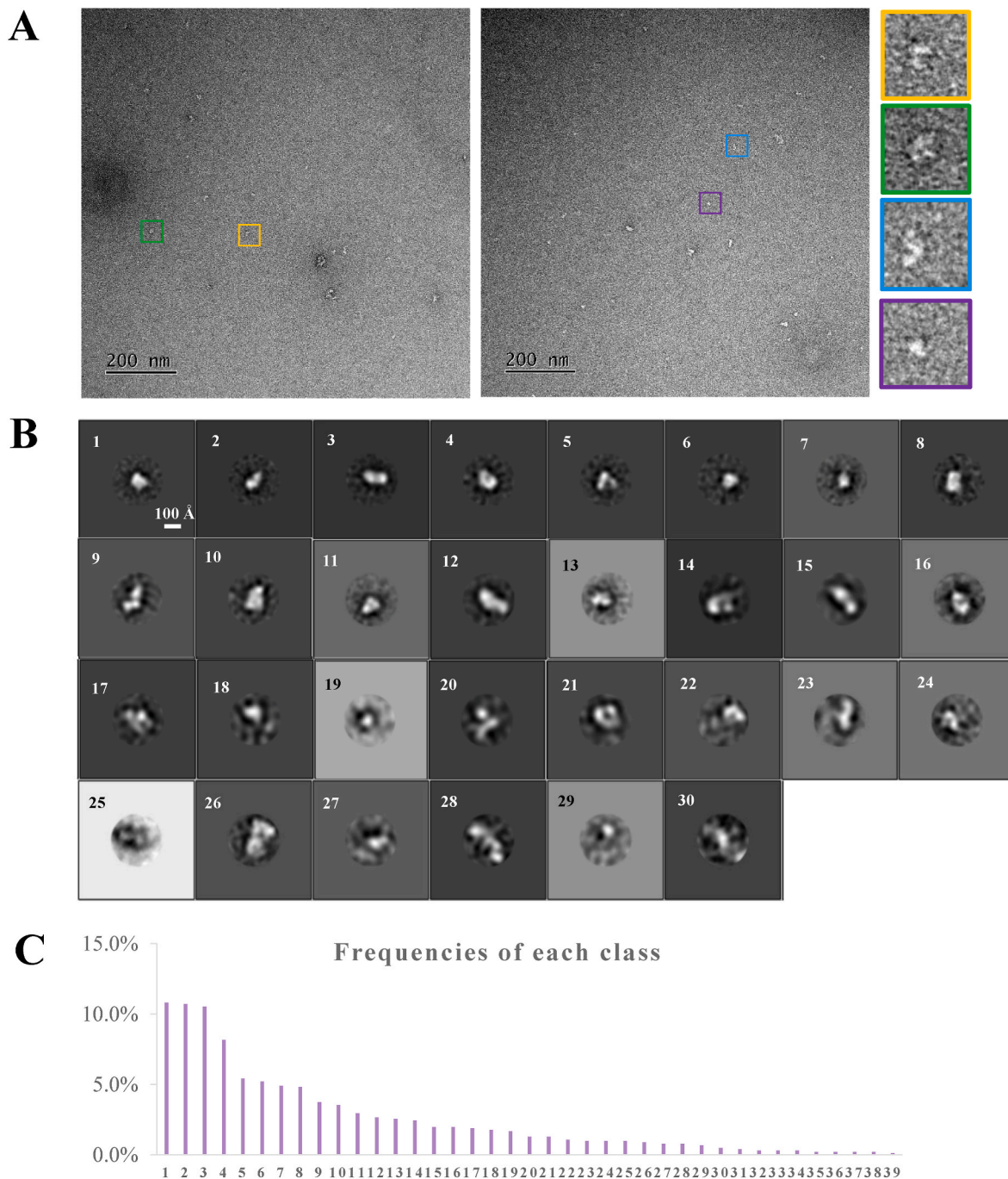
Fig. 7. Negative stain electron microscope images of GPVI/FcRγ SMALP, and 2D class averages from picked particles.
(A) GPVI SMALP gel filtration fraction 7 from Fig. 5 was diluted 10-fold in SMALPing buffer and subjected to negative stain EM. Two representative images are shown. The coloured squares in the images were shown enlarged as representative particles of interest. (B) Single particles from the negative stain EM images were picked, aligned and grouped into 2D class averages using RELION. 50 classes were requested and 39 classes were produced; they were numbered 1–39 with descending amount of particles in their corresponding classes. The averages from the first 30 class averages are shown; the last 9 class averages were either too blurry or of an unusual shape that is unlikely to represent GPVI/FcRγ SMALPs. The scale bar is only shown in class 1, but it is the same for all classes. (C) Frequencies of particles in different classes.

phenomenon on purified SMALPs has been observed in a recently published study, in which over-expressed tetraspanin CD81 was extracted into SMALPs and purified [37]. In that study, the SEC profile comprised two peaks, both containing natively folded CD81, but only the second peak, which may represent CD81 monomer, was functional in binding partner proteins. The authors speculated that the first peak may comprise the oligomers of CD81, or dimerised SMALP discs, and therefore, the binding sites could have been sterically blocked [37]. The SEC profile presented in the present study indicated that, in addition to the two major populations which are more homogeneous, the purified GPVI/FcRγ SMALPs here may comprise additional populations with intermediate sizes. This could possibly reflect the different oligomerisation and clustering status of GPVI/FcRγ in the HEK-293T cell line. Indeed, it is well established on platelets that GPVI/FcRγ clustering on collagen fibres is important for activation [38–41]. It could also be an over-expression phenomenon, such that GPVI density on the cell surface
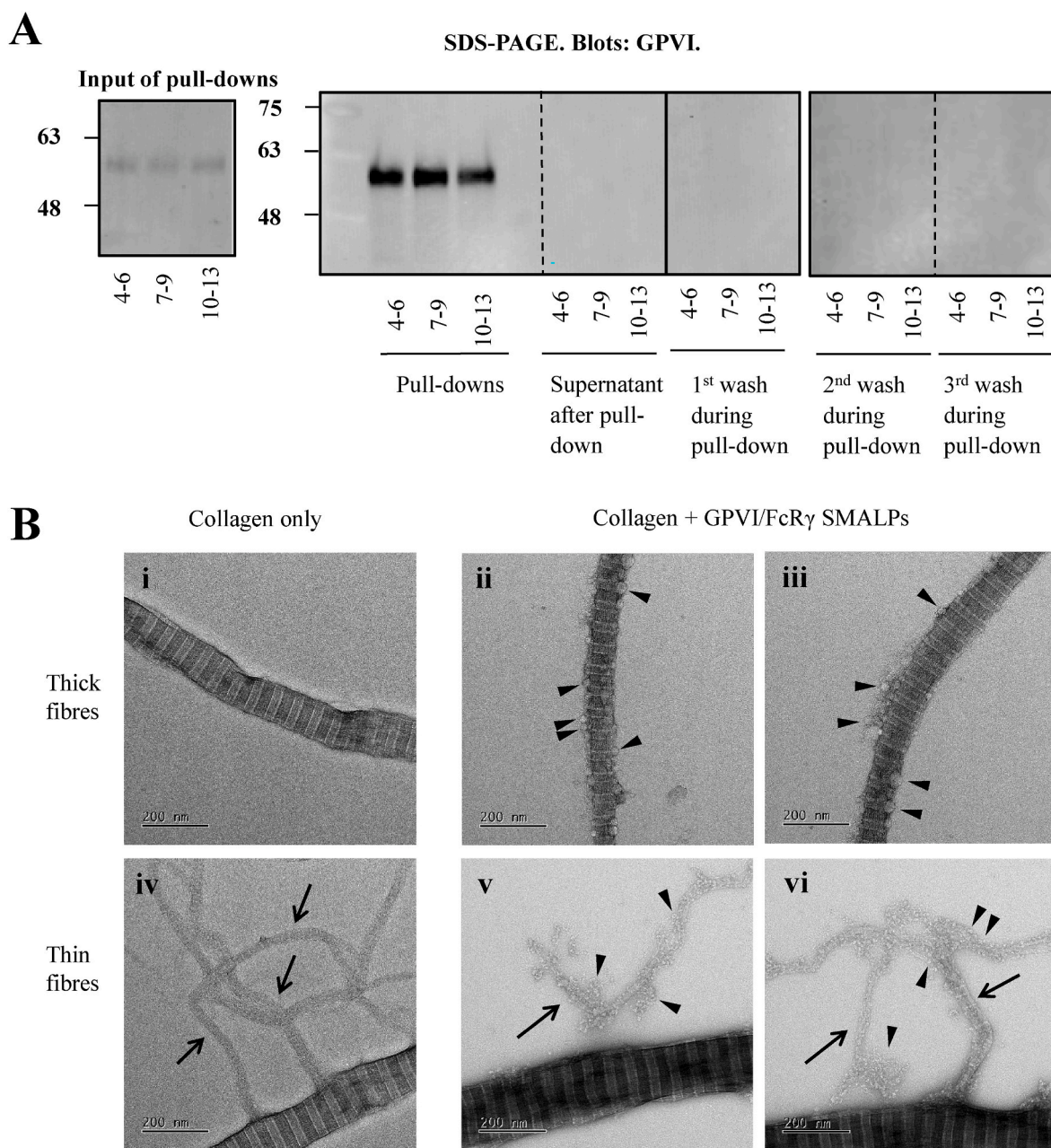
Fig. 8. GPVI/FcRγ SMALPs bind collagen.

(A) The GPVI/FcRγ SMALP gel filtration fractions from Fig. 5 were pooled as indicated, and subjected to collagen-agarose pulldown assay followed by GPVI Western blotting. Dashed lines were used to separate different parts of the blot for clarity. The solid line in the middle of the blot indicates that different parts of the same gel were grouped together on the image. Images from different gels are separately displayed. (B) Horm collagen in SMALP solution was applied onto the grid directly (i and v), or mixed with GPVI/FcRγ SMALPs and then applied onto the grid (ii-iii, v-vi), then subjected to negative stain EM. The final concentration of Horm was 20 μg/mL. Representative nanodiscs, potentially SMALPs, were indicated by black triangles. Thin collagen fibres were indicated by arrows.

is so high that GPVI molecules cluster spontaneously in the absence of GPVI agonists. Indeed, it has been shown that dimerisation for GPVI and another platelet-expressing receptor, CLEC-2, is increased with increasing receptor expression [15,42]. However, given that the collagen pull-down study and negative stain EM images have confirmed the collagen-binding capacity of GPVI in SMALPs, which indicated properly-folded GPVI, the expression system may have captured a wide range of different oligomeric states of the GPVI/FcRγ complex, which could ultimately help to explain the molecular mechanisms of GPVI dimerisation and clustering, and how these events are related to GPVI-agonist-induced platelet activation.

The work here also featured the application of one relatively new native PAGE method, SMA-PAGE, which was specifically developed for SMALPs [25]. SMA-PAGE utilises the unique negatively charged belt, the SMA polymer, as the driving force in PAGE, instead of the traditional SDS, thus the migration of particles on PAGE can be achieved in native sample buffer without heating, preventing the proteins from being denatured and enabling the intact SMALP to migrate during electrophoresis. SMA-PAGE followed by anti-GPVI and anti-FcRγ Western blotting here demonstrated the molecular weight distribution of purified SMALPs, with the molecular weights of protein bands decreasing progressively from the early to later fractions, corresponding with the SEC peak profile. Moreover, relatively little amount of sample is needed in SMA-PAGE, in comparison to many other biophysical characterisations.

As such, SMA-PAGE is an efficient and promising method for identifying the size of GPVI/FcRγ and potentially other receptor complexes in SMALPs. However, further investigation may be needed to distinguish between oligomers encapsulated in SMALPs and SMALPs that aggregate together.

The purified GPVI/FcRγ SMALPs were functional in binding collagen, and GPVI and FcRγ were identified as the main protein components by mass spectrometry. In addition, negative stain EM identified mono-dispersed particles, with sizes comparable to SMALPs and several 2D class averages generated. However, the amount of particles selected for 2D classification was approximately 1,000, which was too low for 3D structure construction. The protein concentration was below 0.1 mg/mL, as measured by three methods: Coomassie-stained SDS-PAGE with the samples in comparison with BSA standards, anti-GPVI Western blotting on samples in comparison with recombinant GPVI-Fc protein, and Nanodrop (data not shown), suggesting an insufficient yield for further biophysical characterisation and structural determination. Furthermore, silver staining on SEC fractions of purified SMALPs still showed multiple visible bands which were not at the sizes of GPVI or FcRγ (Fig. 6), and the anti-His-tag Western blot on the same fractions also showed several additional protein bands apart from the ~57 kDa GPVI monomer band and the ~110 kDa GPVI dimer band (Supplementary Fig. 2). In future, for high-resolution structure determination, a larger amount of purer protein sample is needed, which could be achieved by the use of suspension HEK-293T cells stably expressing GPVI and FcRγ, which can generate higher yields of GPVI/FcRγ complex, and strategies to improve protein purification such as use of two affinity tags.

It has been of debate whether the dimeric form of GPVI represents a unique conformation for ligand binding. Ligand binding studies, with an emphasis on collagen and fibrin(ogen) binding, have generated contradictory results. Originally, Miura et al. showed that fibrous collagen binds to the dimeric form, but not the monomeric form of GPVI, as the recombinant GPVI-Fc protein (the extracellular domain of GPVI fused with dimeric human Fc) inhibited collagen-induced platelet aggregation, but the recombinant monomeric GPVIex protein (the extracellular domain of GPVI) did not [43]. The dimer-specific conformation idea was later reinforced by several dimer-specific antibodies, namely m-Fab-F, 204-11 and 9E18 [44–46]. A few more recent findings, however, challenged the "active dimer" idea, where recombinant monomeric GPVI was shown to bind immobilised collagen by surface plasmon resonance and ELISA, although with lower affinity than recombinant dimeric GPVI [47,48]. Moreover, the deletion of the D2 domain of GPVI, shown to be crucial for GPVI dimerisation, did not abolish GPVI signalling in a transfected B cell line [15]. Bioluminescence resonance energy transfer (BRET) studies showed that GPVI existed as a mixture of monomer, dimer and higher order oligomers in transfected cell lines, and at least partially dimers on resting platelets [15,49]. These findings have questioned the functional significance of GPVI dimer.

Current structural information on GPVI is limited, with the original GPVI structure (without ligand) and a recent structure (with CRP) showing back-to-back dimers, and inhibitory nanobody-bound structures showing either a domain-swapped dimer or a monomer [11–14]. These structures are all crystal structures of the D1 and D2 domains of GPVI. Not only do they lack the structural information in other parts of GPVI, but they also generated contradictory insights into the dimeric interface. In addition, an earlier report showed that human GPVI can dimerise through a disulphide bond at C338 in its intracellular tail, though its functional significance was not determined and its importance questionable in other species because this cysteine residue is not conserved in mice [36]. As this disulphide-linked GPVI dimer was observed within 10–30 s of stimulation by the GPVI-activating snake venom toxin convulxin, the authors suggested that GPVI dimers mediated by extracellular domain interaction pre-exist on the platelet surface, so that the disulphide linking in their cytoplasmic domains can happen rapidly following agonist binding [36]. Therefore, this data suggests that regions of GPVI outside of the D1 and D2 domains may play a role in GPVI dimerisation and potentially clustering. In the original GPVI D1-D2 dimer crystal structure, the same construct failed to dimerise when suspended in solution; however, as stated by the authors, the missing stalk regions may help to stabilise receptor dimerisation, as in the case of the C-type lectin receptor CD94, for example, and the association affinity on the 2D cell membrane could be higher than the 3D space in solution [11,50,51]. Taken together, the structurally unsolved region of GPVI could play important physiological roles, and a full-length GPVI structure, ideally in complex with FcRγ, may provide essential information with regards to GPVI stoichiometry, ligand-binding mode and mechanisms of downstream signalling.

GPVI/FcRγ encapsulated in SMALPs could be an ideal solution for full-length GPVI structure determination. The number of membrane protein structures solved in SMALPs has increased substantially in the last few years. For example, the platelet GPIb-IX-V receptor complex, which plays an important role in haemostasis by binding to von Willebrand factor and other ligands, was recently purified in SMALPs and a low-resolution cryo-EM structure determined [52]. Moreover, for certain membrane proteins, their conformational diversity was better preserved when using SMALPs than when using other membrane protein solubilising methods. For example, the structure of glycine receptor (GlyR) in its partial agonist-binding state was resolved for the first time in SMALPs, revealing open, expanded-open and desensitised states of the receptor, while the membrane scaffold protein (MSP)-nanodisc-encapsulated GlyR only revealed one structure in its desensitised-like state. This suggests that the MSP nanodiscs may have imposed more mobility constraints on, or shifted the conformational equilibrium of the receptor, in comparison to SMALPs [53]. A GPVI/FcRγ SMALP structure could address how regions other than the D1 and D2 domains influence GPVI stoichiometry, and how the receptor complex is configured when inserted in a lipid bilayer.

For high-resolution structure determination of the GPVI/FcRγ complex in SMALPs, it would be ideal to obtain more homogeneous samples, representing one or two oligomerisation states, rather than a series of different order oligomers shown in this current work. Furthermore, it could be beneficial to "lock" the GPVI/FcRγ complex in a specific oligomerisation state by incubating the isolated membrane with multivalent GPVI ligands, for example, dimeric or tetrameric nanobodies of GPVI [39,54], which have well-defined valency in contrast to other multivalent ligands such as collagen, CRP and convulxin. Such efforts could substantially increase the proportion of GPVI/FcRγ complexes in a certain oligomeric state (i.e. GPVI/FcRγ dimer for dimeric nanobodies, GPVI/FcRγ tetramer for tetrameric nanobodies), while the binding of multimeric nanobodies to the GPVI/FcRγ complex could also increase the overall size of the isolated SMALPs, which is beneficial for cryo-EM structure determination. Importantly, such structural knowledge could lead to novel therapeutic strategies to inhibit unwanted GPVI/FcRγ-induced platelet activation in thrombotic diseases.

CRediT authorship contribution statement

Xueqing Wang: Writing – review & editing, Writing – original draft, Validation, Project administration, Methodology, Investigation, Formal analysis, Data curation, Conceptualization. **Alexandre Slater:** Writing – review & editing, Validation, Investigation, Data curation. **Sarah C. Lee:** Writing – review & editing, Resources, Methodology, Data curation. **Neale Harrison:** Data curation. **Naomi L. Pollock:** Methodology, Data curation. **Saskia E. Bakker:** Software, Resources, Methodology, Formal analysis, Data curation. **Stefano Navarro:** Writing – review & editing, Resources. **Bernhard Nieswandt:** Resources. **Tim R. Dafforn:** Resources, Methodology, Conceptualization. **Ángel García:** Writing – review & editing, Supervision, Project administration, Funding acquisition, Data curation. **Steve P. Watson:** Writing – review & editing, Supervision, Project administration, Funding acquisition, Conceptualization. **Michael G. Tomlinson:** Writing – review & editing, Validation, Supervision, Project administration, Methodology, Investigation,

Funding acquisition, Conceptualization.

Acknowledgements

Appendix A. Supplementary data

Supplementary data to this article can be found online at https://doi.org/10.1016/j.abb.2024.109944.

References

[1] J. Rayes, S.P. Watson, B. Nieswandt, Functional significance of the platelet immune receptors GPVI and CLEC-2, J. Clin. Invest. 129 (1) (2019) 12–23, https://doi.org/10.1172/JCI122955.

[2] G. Perrella, M. Nagy, S.P. Watson, J.W.M. Heemskerk, Platelet GPVI (glycoprotein VI) and thrombotic complications in the venous system, Arterioscler. Thromb. Vasc. Biol. 41 (11) (2021) 2681–2692, https://doi.org/10.1161/ATVBAHA.121.316108.

[3] M. Gawaz, Novel ligands for platelet glycoprotein VI, Thromb. Haemostasis 118 (3) (2018) 435–436, https://doi.org/10.1055/s-0038-1635080.

[4] C. Voors-Pette, K. Lebozec, P. Dogterom, L. Jullien, P. Billiald, P. Ferlan, L. Renaud, O. Favre-Bulle, G. Avenard, M. Machacek, Y. Pletan, M. Jandrot-Perrus, Safety and tolerability, pharmacokinetics, and pharmacodynamics of ACT017, an antiplatelet GPVI (glycoprotein VI) fab, Arterioscler. Thromb. Vasc. Biol. 39 (5) (2019) 956–964, https://doi.org/10.1161/ATVBAHA.118.312314.

[5] S. Lockyer, K. Okuyama, S. Begum, S. Le, B. Sun, T. Watanabe, Y. Matsumoto, M. Yoshitake, J. Kambayashi, N.N. Tandon, GPVI-deficient mice lack collagen responses and are protected against experimentally induced pulmonary thromboembolism, Thromb. Res. 118 (3) (2006) 371–380, https://doi.org/10.1016/j.thromres.2005.08.001.

[6] M. Bender, I. Hagedorn, B. Nieswandt, Genetic and antibody-induced glycoprotein VI deficiency equally protects mice from mechanically and FeCl(3) -induced thrombosis, J. Thromb. Haemostasis 9 (7) (2011) 1423–1426, https://doi.org/10.1111/j.1538-7836.2011.04328.x.

[7] V. Matus, G. Valenzuela, C.G. Saez, P. Hidalgo, M. Lagos, E. Aranda, O. Panes, J. Pereira, X. Pillois, A.T. Nurden, D. Mezzano, An adenine insertion in exon 6 of human GP6 generates a truncated protein associated with a bleeding disorder in four Chilean families, J. Thromb. Haemostasis 11 (9) (2013) 1751–1759, https://doi.org/10.1111/jth.12334.

[8] M. Nagy, G. Perrella, A. Dalby, M.F. Becerra, L. Garcia Quintanilla, J.A. Pike, N.V. Morgan, E.E. Gardiner, J.W.M. Heemskerk, L. Azocar, J.F. Miquel, D. Mezzano, S.P. Watson, Flow studies on human GPVI-deficient blood under coagulating and noncoagulating conditions, Blood Adv. 4 (13) (2020) 2953–2961, https://doi.org/10.1182/bloodadvances.2020001761.

[9] M. Moroi, S.M. Jung, Platelet glycoprotein VI: its structure and function, Thromb. Res. 114 (4) (2004) 221–233, https://doi.org/10.1016/j.thromres.2004.06.046.

[10] Y.M. Zheng, C. Liu, H. Chen, D. Locke, J.C. Ryan, M.L. Kahn, Expression of the platelet receptor GPVI confers signaling via the Fc receptor gamma -chain in response to the snake venom convulxin but not to collagen, J. Biol. Chem. 276 (16) (2001) 12999–13006, https://doi.org/10.1074/jbc.M009344200.

[11] K. Horii, M.L. Kahn, A.B. Herr, Structural basis for platelet collagen responses by the immune-type receptor glycoprotein VI, Blood 108 (3) (2006) 936–942, https://doi.org/10.1182/blood-2006-01-010215.

[12] A. Slater, Y. Di, J.C. Clark, N.J. Jooss, E.M. Martin, F. Alenazy, M.R. Thomas, R.A. S. Ariens, A.B. Herr, N.S. Poulter, J. Emsley, S.P. Watson, Structural characterization of a novel GPVI-nanobody complex reveals a biologically active domain-swapped GPVI dimer, Blood 137 (24) (2021) 3443–3453, https://doi.org/10.1182/blood.2020009440.

[13] L.J. Feitsma, H.C. Brondijk, G.E. Jarvis, D. Hagemans, D. Bihan, N. Jerah, M. Versteeg, R.W. Farndale, E.G. Huizinga, Structural insights into collagen binding by platelet receptor glycoprotein VI, Blood 139 (20) (2022) 3087–3098, https://doi.org/10.1182/blood.2021013614.

[14] F.N. Damaskinaki, N.J. Jooss, E.M. Martin, J.C. Clark, M.R. Thomas, N.S. Poulter, J. Emsley, B. Kellam, S.P. Watson, A. Slater, Characterizing the binding of glycoprotein VI with nanobody 35 reveals a novel monomeric structure of glycoprotein VI where the conformation of D1+D2 is independent of dimerization, J. Thromb. Haemostasis 21 (2) (2023) 317–328, https://doi.org/10.1016/j.jtha.2022.11.002.

[15] J.C. Clark, R.A.I. Neagoe, M. Zuidscherwoude, D.M. Kavanagh, A. Slater, E. M. Martin, M. Soave, D. Stegner, B. Nieswandt, N.S. Poulter, J. Hummert, D. P. Herten, M.G. Tomlinson, S.J. Hill, S.P. Watson, Evidence that GPVI is expressed as a mixture of monomers and dimers, and that the D2 domain is not essential for GPVI activation, Thromb. Haemostasis 121 (11) (2021) 1435–1447, https://doi.org/10.1055/a-1401-5014.

[16] J.C. Clark, F.N. Damaskinaki, Y.F.H. Cheung, A. Slater, S.P. Watson, Structure-function relationship of the platelet glycoprotein VI (GPVI) receptor: does it matter if it is a dimer or monomer? Platelets 32 (6) (2021) 724–732, https://doi.org/10.1080/09537104.2021.1887469.

[17] A. Slater, G. Perrella, M.B. Onselaer, E.M. Martin, J.S. Gauer, R.G. Xu, J. W. Heemskerk, R.A.S. Ariens, S.P. Watson, Does fibrin(ogen) bind to monomeric or dimeric GPVI, or not at all? Platelets (2018) 1–9, https://doi.org/10.1080/09537104.2018.1508649.

[18] J.M. Dorr, S. Scheidelaar, M.C. Koorengevel, J.J. Dominguez, M. Schafer, C.A. van Walree, J.A. Killian, The styrene-maleic acid copolymer: a versatile tool in membrane research, Eur. Biophys. J. 45 (1) (2016) 3–21, https://doi.org/10.1007/s00249-015-1093-y.

[19] S.C. Lee, T.J. Knowles, V.L. Postis, M. Jamshad, R.A. Parslow, Y.P. Lin, A. Goldman, P. Sridhar, M. Overduin, S.P. Muench, T.R. Dafforn, A method for detergent-free isolation of membrane proteins in their local lipid environment, Nat. Protoc. 11 (7) (2016) 1149–1162, https://doi.org/10.1038/nprot.2016.070.

[20] T.J. Knowles, R. Finka, C. Smith, Y.P. Lin, T. Dafforn, M. Overduin, Membrane proteins solubilized intact in lipid containing nanoparticles bounded by styrene maleic acid copolymer, J. Am. Chem. Soc. 131 (22) (2009) 7484–7485, https://doi.org/10.1021/ja810046q.

[21] B. Krishnarjuna, A. Ramamoorthy, Detergent-Free isolation of membrane proteins and strategies to study them in a near-native membrane environment, Biomolecules 12 (8) (2022), https://doi.org/10.3390/biom12081076.

[22] M.G. Tomlinson, S.D. Calaminus, O. Berlanga, J.M. Auger, T. Bori-Sanz, L. Meyaard, S.P. Watson, Collagen promotes sustained glycoprotein VI signaling in platelets and cell lines, J. Thromb. Haemostasis 5 (11) (2007) 2274–2283, https://doi.org/10.1111/j.1538-7836.2007.02746.x.

[23] C.Z. Koo, N. Harrison, P.J. Noy, J. Szyroka, A.L. Matthews, H.E. Hsia, S.A. Muller, J. Tushaus, J. Goulding, K. Willis, C. Apicella, B. Cragoe, E. Davis, M. Keles, A. Malinova, T.A. McFarlane, P.R. Morrison, H.T.H. Nguyen, M.C. Sykes, H. Ahmed, A. Di Maio, L. Seipold, P. Saftig, E. Cull, C. Pliotas, E. Rubinstein, N. S. Poulter, S.J. Briddon, N.D. Holliday, S.F. Lichtenthaler, M.G. Tomlinson, The tetraspanin Tspan15 is an essential subunit of an ADAM10 scissor complex, J. Biol. Chem. 295 (36) (2020) 12822–12839, https://doi.org/10.1074/jbc.RA120.012601.

[24] P.J. Noy, P. Lodhia, K. Khan, X. Zhuang, D.G. Ward, A.R. Verissimo, A. Bacon, R. Bicknell, Blocking CLEC14A-MMRN2 binding inhibits sprouting angiogenesis and tumour growth, Oncogene 34 (47) (2015) 5821–5831, https://doi.org/10.1038/onc.2015.34.

[25] N.L. Pollock, M. Rai, K.S. Simon, S.J. Hesketh, A.C.K. Teo, M. Parmar, P. Sridhar, R. Collins, S.C. Lee, Z.N. Stroud, S.E. Bakker, S.P. Muench, C.H. Barton, G. Hurlbut, D.I. Roper, C.J.I. Smith, T.J. Knowles, C.M. Spickett, J.M. East, V.L.G. Postis, T. R. Dafforn, SMA-PAGE: a new method to examine complexes of membrane proteins using SMALP nano-encapsulation and native gel electrophoresis, Biochim. Biophys. Acta Biomembr. 1861 (8) (2019) 1437–1445, https://doi.org/10.1016/j.bbamem.2019.05.011.

[26] M. Al-Tamimi, F.T. Mu, J.F. Arthur, Y. Shen, M. Moroi, M.C. Berndt, R.K. Andrews, E.E. Gardiner, Anti-glycoprotein VI monoclonal antibodies directly aggregate platelets independently of FcgammaRIIa and induce GPVI ectodomain shedding, Platelets 20 (2) (2009) 75–82, https://doi.org/10.1080/09537100802645029.

[27] S. Navarro, D. Stegner, B. Nieswandt, J.W.M. Heemskerk, M.J.E. Kuijpers, Temporal roles of platelet and coagulation pathways in collagen- and tissue factor-induced thrombus formation, Int. J. Mol. Sci. 23 (1) (2021), https://doi.org/10.3390/ijms23010358.

[28] J. Zivanov, T. Nakane, B.O. Forsberg, D. Kimanius, W.J. Hagen, E. Lindahl, S. H. Scheres, New tools for automated high-resolution cryo-EM structure determination in RELION-3, Elife 7 (2018), https://doi.org/10.7554/eLife.42166.

[29] A.R. Sarhan, T.R. Patel, A.J. Creese, M.G. Tomlinson, C. Hellberg, J.K. Heath, N. A. Hotchin, D.L. Cunningham, Regulation of platelet derived growth factor signaling by leukocyte common antigen-related (LAR) protein tyrosine phosphatase: a quantitative phosphoproteomics study, Mol. Cell. Proteomics 15 (6) (2016) 1823–1836, https://doi.org/10.1074/mcp.M115.053652.

[30] L. Joutsi-Korhonen, P.A. Smethurst, A. Rankin, E. Gray, I.J. M, C.M. Onley, N. A. Watkins, L.M. Williamson, A.H. Goodall, P.G. de Groot, R.W. Farndale, W. H. Ouwehand, The low-frequency allele of the platelet collagen signaling receptor glycoprotein VI is associated with reduced functional responses and expression, Blood 101 (11) (2003) 4372–4379, https://doi.org/10.1182/blood-2002-08-2591.

[31] C.I. Jones, S.F. Garner, W. Angenent, A. Bernard, C. Berzuini, P. Burns, R. W. Farndale, J. Hogwood, A. Rankin, J.C. Stephens, B.D. Tom, J. Walton, F. Dudbridge, W.H. Ouwehand, A.H. Goodall, C. Bloodomics, Mapping the platelet profile for functional genomic studies and demonstration of the effect size of the GP6 locus, J. Thromb. Haemostasis 5 (8) (2007) 1756–1765, https://doi.org/10.1111/j.1538-7836.2007.02632.x.

[32] E. Trifiro, S.A. Williams, Y. Cheli, K. Furihata, F.M. Pulcinelli, D.J. Nugent, T. J. Kunicki, The low-frequency isoform of platelet glycoprotein VIb attenuates ligand-mediated signal transduction but not receptor expression or ligand binding, Blood 114 (9) (2009) 1893–1899, https://doi.org/10.1182/blood-2009-03-209510.

[33] A. Asfari, J.A. Dent, A. Corken, D. Herington, V. Kaliki, N. Sra, G. Hefley, S. Pasala, P. Prodhan, J. Ware, Platelet glycoprotein VI haplotypes and the presentation of

paediatric sepsis, Thromb. Haemostasis 119 (3) (2019) 431–438, https://doi.org/10.1055/s-0038-1676794.

[34] C. Steentoft, S.Y. Vakhrushev, H.J. Joshi, Y. Kong, M.B. Vester-Christensen, K.T.B. G. Schjoldager, K. Lavrsen, S. Dabelsteen, N.B. Pedersen, L. Marcos-Silva, R. Gupta, E.P. Bennett, U. Mandel, S. Brunak, H.H. Wandall, S.B. Levery, H. Clausen, Precision mapping of the human -GalNAc glycoproteome through SimpleCell technology, EMBO J. 32 (10) (2013) 1478–1488, https://doi.org/10.1038/emboj.2013.79.

[35] P.J. Noy, J. Yang, J.S. Reyat, A.L. Matthews, A.E. Charlton, J. Furmston, D. A. Rogers, G.E. Rainger, M.G. Tomlinson, TspanC8 tetraspanins and A disintegrin and metalloprotease 10 (ADAM10) interact via their extracellular regions: evidence for distinct binding mechanisms for different TspanC8 proteins, J. Biol. Chem. 291 (7) (2016) 3145–3157, https://doi.org/10.1074/jbc.M115.703058.

[36] J.F. Arthur, Y. Shen, M.L. Kahn, M.C. Berndt, R.K. Andrews, E.E. Gardiner, Ligand binding rapidly induces disulfide-dependent dimerization of glycoprotein VI on the platelet plasma membrane, J. Biol. Chem. 282 (42) (2007) 30434–30441, https://doi.org/10.1074/jbc.M701330200.

[37] H. Ayub, M. Clare, I. Milic, N.P. Chmel, H. Boning, A. Devitt, T. Krey, R.M. Bill, A. J. Rothnie, CD81 extracted in SMALP nanodiscs comprises two distinct protein populations within a lipid environment enriched with negatively charged headgroups, Biochim. Biophys. Acta Biomembr. 1862 (11) (2020) 183419, https://doi.org/10.1016/j.bbamem.2020.183419.

[38] N.J. Jooss, C.W. Smith, A. Slater, S.J. Montague, Y. Di, C. O'Shea, M.R. Thomas, Y. M.C. Henskens, J.W.M. Heemskerk, S.P. Watson, N.S. Poulter, Anti-GPVI nanobody blocks collagen- and atherosclerotic plaque-induced GPVI clustering, signaling, and thrombus formation, J. Thromb. Haemostasis 20 (11) (2022) 2617–2631, https://doi.org/10.1111/jth.15836.

[39] Z. Maqsood, J.C. Clark, E.M. Martin, Y.F.H. Cheung, L.A. Moran, S.E.T. Watson, J. A. Pike, Y. Di, N.S. Poulter, A. Slater, B.M.H. Lange, B. Nieswandt, J.A. Eble, M. G. Tomlinson, D.M. Owen, D. Stegner, L.J. Bridge, C. Wierling, S.P. Watson, Experimental validation of computerised models of clustering of platelet glycoprotein receptors that signal via tandem SH2 domain proteins, PLoS Comput. Biol. 18 (11) (2022) e1010708, https://doi.org/10.1371/journal.pcbi.1010708.

[40] C. Pallini, J.A. Pike, C. O'Shea, R.K. Andrews, E.E. Gardiner, S.P. Watson, N. S. Poulter, Immobilized collagen prevents shedding and induces sustained GPVI clustering and signaling in platelets, Platelets 32 (1) (2021) 59–73, https://doi.org/10.1080/09537104.2020.1849607.

[41] N.S. Poulter, A.Y. Pollitt, D.M. Owen, E.E. Gardiner, R.K. Andrews, H. Shimizu, D. Ishikawa, D. Bihan, R.W. Farndale, M. Moroi, S.P. Watson, S.M. Jung, Clustering of glycoprotein VI (GPVI) dimers upon adhesion to collagen as a mechanism to regulate GPVI signaling in platelets, J. Thromb. Haemostasis 15 (3) (2017) 549–564, https://doi.org/10.1111/jth.13613.

[42] J.C. Clark, E.M. Martin, L.A. Moran, Y. Di, X. Wang, M. Zuidscherwoude, H. C. Brown, D.M. Kavanagh, J. Hummert, J.A. Eble, B. Nieswandt, D. Stegner, A. Y. Pollitt, D.P. Herten, M.G. Tomlinson, A. Garcia, S.P. Watson, Divalent nanobodies to platelet CLEC-2 can serve as agonists or antagonists, Commun. Biol. 6 (1) (2023) 376, https://doi.org/10.1038/s42003-023-04766-6.

[43] Y. Miura, T. Takahashi, S.M. Jung, M. Moroi, Analysis of the interaction of platelet collagen receptor glycoprotein VI (GPVI) with collagen. A dimeric form of GPVI, but not the monomeric form, shows affinity to fibrous collagen, J. Biol. Chem. 277 (48) (2002) 46197–46204, https://doi.org/10.1074/jbc.M204029200.

[44] S.M. Jung, M. Moroi, K. Soejima, T. Nakagaki, Y. Miura, M.C. Berndt, E. E. Gardiner, J.M. Howes, N. Pugh, D. Bihan, S.P. Watson, R.W. Farndale, Constitutive dimerization of glycoprotein VI (GPVI) in resting platelets is essential for binding to collagen and activation in flowing blood, J. Biol. Chem. 287 (35) (2012) 30000–30013, https://doi.org/10.1074/jbc.M112.359125.

[45] S.M. Jung, K. Tsuji, M. Moroi, Glycoprotein (GP) VI dimer as a major collagen-binding site of native platelets: direct evidence obtained with dimeric GPVI-specific Fabs, J. Thromb. Haemostasis 7 (8) (2009) 1347–1355, https://doi.org/10.1111/j.1538-7836.2009.03496.x.

[46] S. Loyau, B. Dumont, V. Ollivier, Y. Boulaftali, L. Feldman, N. Ajzenberg, M. Jandrot-Perrus, Platelet glycoprotein VI dimerization, an active process inducing receptor competence, is an indicator of platelet reactivity, Arterioscler. Thromb. Vasc. Biol. 32 (3) (2012) 778–785, https://doi.org/10.1161/ATVBAHA.111.241067.

[47] R.G. Xu, J.S. Gauer, S.R. Baker, A. Slater, E.M. Martin, H.R. McPherson, C. Duval, I. W. Manfield, A.M. Bonna, S.P. Watson, R.A.S. Ariens, GPVI (glycoprotein VI) interaction with fibrinogen is mediated by avidity and the fibrinogen alphaC-region, Arterioscler. Thromb. Vasc. Biol. 41 (3) (2021) 1092–1104, https://doi.org/10.1161/ATVBAHA.120.315030.

[48] M.B. Onselaer, A.T. Hardy, C. Wilson, X. Sanchez, A.K. Babar, J.L.C. Miller, C. N. Watson, S.K. Watson, A. Bonna, H. Philippou, A.B. Herr, D. Mezzano, R.A. S. Ariens, S.P. Watson, Fibrin and D-dimer bind to monomeric GPVI, Blood Adv. 1 (19) (2017) 1495–1504, https://doi.org/10.1182/bloodadvances.2017007732.

[49] O. Berlanga, T. Bori-Sanz, J.R. James, J. Frampton, S.J. Davis, M.G. Tomlinson, S. P. Watson, Glycoprotein VI oligomerization in cell lines and platelets, J. Thromb. Haemostasis 5 (5) (2007) 1026–1033, https://doi.org/10.1111/j.1538-7836.2007.02449.x.

[50] H. Chen, D. Locke, Y. Liu, C. Liu, M.L. Kahn, The platelet receptor GPVI mediates both adhesion and signaling responses to collagen in a receptor density-dependent fashion, J. Biol. Chem. 277 (4) (2002) 3011–3019, https://doi.org/10.1074/jbc.M109714200.

[51] J.C. Boyington, A.N. Raiz, A.G. Brooks, A. Patamawenu, P.D. Sun, Reconstitution of bacterial expressed human CD94: the importance of the stem region for dimer formation, Protein Expr. Purif. 18 (2) (2000) 235–241, https://doi.org/10.1006/prep.1999.1188.

[52] J. Lu, C. Zhang, S. Shi, S. Li, J. Liu, J. Wu, C. Huang, M. Lei, Stoichiometry and architecture of the platelet membrane complex glycoprotein Ib-IX-V, Biol. Chem. (2023), https://doi.org/10.1515/hsz-2022-0227.

[53] J. Yu, H. Zhu, R. Lape, T. Greiner, J. Du, W. Lu, L. Sivilotti, E. Gouaux, Mechanism of gating and partial agonist action in the glycine receptor, Cell 184 (4) (2021) 957–968 e21, https://doi.org/10.1016/j.cell.2021.01.026.

[54] E.M. Martin, J.C. Clark, S.J. Montague, L.A. Moran, Y. Di, L.J. Bull, L. Whittle, F. Raka, R.J. Buka, I. Zafar, C. Kardeby, A. Slater, S.P. Watson, Trivalent nanobody-based ligands mediate powerful activation of GPVI, CLEC-2, and PEAR1 in human platelets whereas FcgammaRIIA requires a tetravalent ligand, J. Thromb. Haemostasis 22 (1) (2024) 271–285, https://doi.org/10.1016/j.jtha.2023.09.026.